Open Research Online

The Open University's repository of research publications
and other research outputs

Emergence of a secondary rainbow and the dynamical polarization potential for ^{16}O on ^{12}C at 330 MeV

Journal Item

oro.open.ac.uk

Emergence of a secondary rainbow and the dynamical polarization potential for ^{16}O on ^{12}C at 330 MeV

R. S. Mackintosh[*]

Department of Physical Sciences, The Open University, Milton Keynes MK7 6AA, United Kingdom

Y. Hirabayashi[†]

Information Initiative Center, Hokkaido University, Sapporo 060-0811, Japan

S. Ohkubo[‡]

Research Center for Nuclear Physics, Osaka University, Ibaraki, Osaka 567-0047, Japan
and University of Kochi, Kochi 780-8515, Japan

Background: It was shown recently that an anomaly in the elastic scattering of ^{16}O on ^{12}C at around 300 MeV is resolved by including within the scattering model the inelastic excitation of specific collective excitations of both nuclei, leading to a secondary rainbow. There is very little systematic knowledge concerning the contribution of collective excitations to the interaction between nuclei, particularly in the overlap region when neither interacting nuclei are light nuclei.

Purpose: Our goals are to study the dynamic polarization potential (DPP) generated by channel coupling that has been experimentally validated for a case (^{16}O on ^{12}C at around 300 MeV) where scattering is sensitive to the nuclear potential over a wide radial range; to exhibit evidence of the nonlocality due to collective coupling; to validate, or otherwise invalidate, the representation of the DPP by uniform renormalizing folding models or global potentials.

Methods: S-matrix to potential, $S_L \rightarrow V(r)$, inversion yields local potentials that reproduce the elastic channel S matrix of coupled channel calculations. Subtracting the elastic channel uncoupled potential yields a local L-independent representation of the DPP. The dependence of the DPP on the nature of the coupled states and other parameters can be studied.

Results: Local DPPs were found due to the excitation of ^{12}C and the combined excitation of ^{16}O and ^{12}C. The radial forms were different for the two cases, but each were very different from a uniform renormalization of the potential. The full coupling led to a 10% increase in the volume integral of the real potential. Evidence for the nonlocality of the underlying formal DPP and for the effect of direct coupling between the collective states is presented.

Conclusions: The local DPP generating the secondary rainbow has been identified. In general, DPPs have forms that depend on the nature of the specific excitations generating them, but, as in this case, they cannot be represented by a uniform renormalization of a global model or folding model potential. The method employed herein is a useful tool for further exploration of the contribution of collective excitations to internuclear potentials, concerning which there is still remarkably little general information.

I. INTRODUCTION

The collective excitation of interacting nuclei strongly influences the elastic scattering between those nuclei. This was clearly demonstrated in Ref. [1] by the discovery of a secondary rainbow in ^{16}O on ^{12}C elastic scattering, resolving a significant anomalous situation involving the elastic scattering of this pair of nuclei. A global model that had proven satisfactory for energies from 62 to 1503 MeV was found to be significantly inadequate when confronted with wide angular range data at $E_L = 281$ MeV. At this and similar energies, the Airy minimum of nuclear rainbow scattering appears at a much larger angle, $\theta \sim 70°$, than expected with the global model. As

described in Ref. [1], this problem was resolved by including excitation of the 2^+ and 3^- states of ^{12}C and the 3^- and 2^+ states of ^{16}O within an extended folding model. Within this model, a secondary nuclear rainbow appears having an Airy minimum at a large angle, consistent with experiment over a range of energies, with the primary rainbow at more forward angles being somewhat obscured. In this way, including the excitation of the various collective states resolves a significant anomaly and leads to an understanding of further phenomena related to nuclear rainbow scattering [2].

The excitation of collective states plays an important role in the dynamics of the interactions between all pairs of nuclei. However, there is little systematic knowledge, particularly for heavy ion scattering, concerning the contribution of such collective states to the scattering potential. In this paper we shall demonstrate a means of mitigating this lack of information. The case we study, ^{16}O on ^{12}C at 330 MeV, is

_____

[*]raymond.mackintosh@open.ac.uk

[†]hirabay@iic.hokudai.ac.jp

[‡]ohkubo@yukawa.kyoto-u.ac.jp

one in which the contribution of collective states has been shown to resolve a known anomaly. The results will throw light on the limitations of standard phenomenology that is based on parameterized forms or based on folding models that lead to smooth potentials. They also suggest a richness of phenomena concerning the dynamics of interacting nuclei, including evidence for dynamically generated nonlocality. The procedure exemplified in this paper is of wide applicability. Section II reviews relevant general properties of the DPP, Sec. III introduces the model and discusses the DPP due to excitations of ^{12}C, Sec. IV presents the effects of excitations of ^{16}O, Sec. V discusses the results and the implications, and Sec. VI briefly summarizes.

II. THE DYNAMIC POLARIZATION POTENTIAL

Within a potential model, the effects of channel coupling can be represented as a dynamic polarization potential, DPP, added to a folding model potential; see Refs. [3,4] for example. The formal DPP is both L dependent and nonlocal, the nonlocality being in addition to that which arises from exchange processes. Adding such a nonlocal, L-dependent potential to the folding model potential yields a potential that is itself nonlocal and L dependent. Such a potential is not easily comparable with local phenomenological potentials; see for example Ref. [5]. However, it is always possible, using $S_L \to V(r)$ inversion, to find a local and L-independent potential that yields the same S matrix, and hence all elastic scattering observables, as any nonlocal and L-dependent potential. In this way, we can determine a potential that exactly reproduces the S matrix of the sum of the formal DPP and the folding model potential. This local potential can be compared with potentials determined by means of precision phenomenological fitting. We shall generally refer to the local DPP found by $S_L \to V(r)$ inversion of the coupled channel S_L, followed by subtraction of the folding model ("bare") potential, as "the DPP." However, when it is relevant that the true, formal DPP [3,4] is nonlocal, we refer to this as the "underlying DPP." We shall present some evidence for that nonlocality.

For the particular case of proton scattering from nuclei, it has been shown [6] that collective excitations give rise to local DPPs that are strongly undulatory. This may be related to the nonlocality and/or L dependence of the underlying formal DPP; specific evidence concerning this nonlocality for proton scattering was presented in Ref. [7]. Less is known about the properties of the DPP for multinucleon projectiles than for nucleons, apart from a few studies for lighter heavy ions and various cases of DPPs generated by projectile breakup. The effects of channel coupling are commonly absorbed into an overall renormalization of a global optical model potential (OMP) or folding model (FM) potential, a practice that we shall comment upon later. This procedure may be justified for those heavy ion reactions for which only the nuclear surface region is significant.

III. THE MODEL AND DPP FOR ^{16}O + ^{12}C SCATTERING

The case of scattering studied here, ^{16}O on ^{12}C at some hundreds of MeV, is characterized by a high degree of

penetration of the two nuclei, so there is some sensitivity at large angles to the potential for almost complete overlap of the two nuclei. This motivates the determination of the DPP over a wide radial range. The coupled channel model of Ref. [1] is much more realistic than earlier models for which DPPs for the same pair of nuclei were calculated [8,9], and is validated by its detailed fit to wide angular range elastic scattering data, solving the problem of the rainbow scattering angle.

For 330 MeV incident energy, a standard double folding (DF) model calculation, with no inelastic coupling, failed to fit beyond about $60°$ elastic scattering differential cross section data extending beyond $90°$. The initial extended double folding (EDF) coupled channel calculation included coupling to the collective 2^+ and 3^- states of ^{12}C at 4.44 and 9.64 MeV respectively. A further calculation ("full") also included the 3^- and 2^+ states of ^{16}O at 6.13 and 6.92 MeV. A Woods-Saxon imaginary term is added to the real DF and EDF interactions. This is shallower for the initial EDF calculations with a further reduction in depth and diffusivity for the full calculation. The DPPs that we present for the initial and full cases are calculated by subtracting the relevant bare (diagonal, uncoupled) potential, with its appropriate imaginary term, from the potential that is found by inversion to reproduce the EDF model elastic channel S matrix. Since the DPP for any given case is somewhat dependent on the imaginary part of the bare potential, this should be borne in mind when comparing the DPPs for the initial and full cases.

We calculated the DPPs for the following four sets of inelastic excitations of ^{12}C, all involving the same initial bare imaginary term: (i) the 2^+ state, (ii) the 3^- state, (iii) the 2^+ and 3^- states with direct coupling between these excited states, and (iv) the 2^+ and 3^- states with no direct coupling between them. We also calculated the DPPs for the full case including the 2^+ and 3^- states of ^{16}O with the relevant imaginary bare potential. In no case was the imaginary potential deformed, so the coupling potential was purely real.

The elastic scattering S matrix from the coupled channel calculation was subjected to $S_L \to V(r)$ inversion using the iterative-perturbative, IP, inversion procedure [10–14]. The resulting potential exactly reproduces the elastic scattering from the coupled channel, CC, calculation. Subtracting the diagonal elastic channel potential from the inverted potential yields a local L-independent representation of the DPP corresponding to whatever particular channels inelastic channels were included in the CC calculation.

It is useful to quantify the DPPs for the various cases in a simple way by subtracting from the volume integrals and rms radii for the inverted potential the same quantities for the bare potentials. This gives the changes that are induced by the coupling. The results are presented in Table I. Specifically, we calculate ΔJ_R, $\Delta R_R(\text{rms})$, ΔJ_I, and $\Delta R_I(\text{rms})$ which are the changes in the real volume integral and rms radius and the imaginary volume integral and rms radius. All volume integrals are conventionally defined in terms of nucleon pairs [4]. The quantities ΔJ_R and ΔJ_I are the volume integrals of the real and imaginary parts of the DPP while the interpretation of the radial quantities is less direct. The quantity ΔJ_R alone gives an incomplete view of the change in the real potential since this typically has both attractive and

TABLE I. For ^{16}O scattering from ^{12}C at 330 MeV, with the characteristics of the DPP due to the coupling specified in column 1; the first 5 rows are for ^{12}C states only. The columns ΔJ_R and ΔJ_I give the change in the volume integral (per nucleon pair) of the real and imaginary components of the DPP induced by the coupling. The columns ΔR_R(rms) and ΔR_I(rms) respectively give the change in rms radius of the real and imaginary central components. Negative ΔJ_R corresponds to repulsion. In line 5, "ndc" indicates no direct coupling between the 2^+ and 3^- states. The two final columns present, respectively, the change in the total reaction cross section induced by the coupling, and the integrated cross section of the specific coupled reaction channels.

Coupling	ΔJ_R (MeV fm^3)	ΔR_R(rms) (fm)	ΔJ_I (MeV fm^3)	ΔR_I(rms) (fm)	Δ CS (mb)	Inel. CS (mb)
2^+	7.67	$-$0.0077	20.68	$-$0.0815	11.8	11.4
3^-	$-$0.34	0.0036	2.37	$-$0.0007	4.3	3.9
2^+ and 3^-	5.85	0.0013	28.56	$-$0.0917	15.6	14.8
$\sum 2^+ 3^-$	7.33	$-$0.0041	23.06	$-$0.0822	16.1	15.3
2^+ and 3^- ndc	6.12	$-$0.0019	25.21	$-$0.0909	15.7	14.9
Full coupling	28.74	$-$0.0064	35.96	0.0106	70.4	57.4

repulsive regions. However since J_R for the bare potential is 278.48 MeV fm^3, it can be seen that for the full case, the attraction due to the coupling corresponds to a 10% increase in the volume integral. In fact there is a 30% increase around 3.5 fm; see Fig. 3 discussed in Sec. IV below.

Insight into the nonlocality of the underlying formal DPP can be gained from a comparison of lines 4 and 5 of Table I based on the fact that the local equivalent of the sum of two nonlocal potentials is not the sum of the local equivalents of each potential. The nonlocal DPPs due to the excitation of two states when there is no direct coupling between those states add to give the nonlocal DPP due to those states. However, the presence of nonlocality is indicated by the nonexact addition of the local equivalent DPPs. Line 4 of Table I gives the numerical sum of the numbers in rows 1 and 2, and we draw attention to the volume integrals which are clearly unequal to the volume integrals in line 5, the case in which the two states are excited with no direct coupling between them. Although not directly related to the issue of underlying nonlocality, it is also of interest to compare lines 3 and 5; it appears that direct coupling between the states somewhat reduces the attractive effect but somewhat increases the absorptive effect of the coupling, with no significant effect on the total inelastic or reaction cross sections.

The bare and inverted potentials for the case with coupling to the 2^+ and 3^- states, with direct coupling between them, are shown in Fig. 1. The dotted line corresponds to the potential quantified in line 3 of Table I and the dashed line corresponds to the slightly less exact fit to S_L of an earlier iteration of the inversion. The development of quite sharp undulations appears to be genuine, and we comment on it later; the volume integrals and other characteristics of the two potentials are quite close. The DPP can be read off as the difference between the dotted line and the solid line representing the bare potential. The attractive nature of the real DPP for $r \leqslant 3.5$ fm, and the emissive character of the imaginary DPP for $r \leqslant 3$ fm, are well determined by the inversion, and are within the radial range within which the scattering out to 90° is sensitive, as verified with notch tests. It was found that somewhat less undulatory potentials could be found if a small Majorana $[(-1)^L]$ term was included in the inversion, but this might have been simulating some other form of L dependence, and this requires further investigation.

The real and imaginary DPPs when the direct coupling between the 2^+ and 3^- states is turned off are similar but somewhat smoother, as can be seen from Fig. 2. In this case it was readily possible to get a very close reproduction of S_L without the sharp undulations seen in Fig. 1. It was possible to get a slightly smoother potential by stopping the
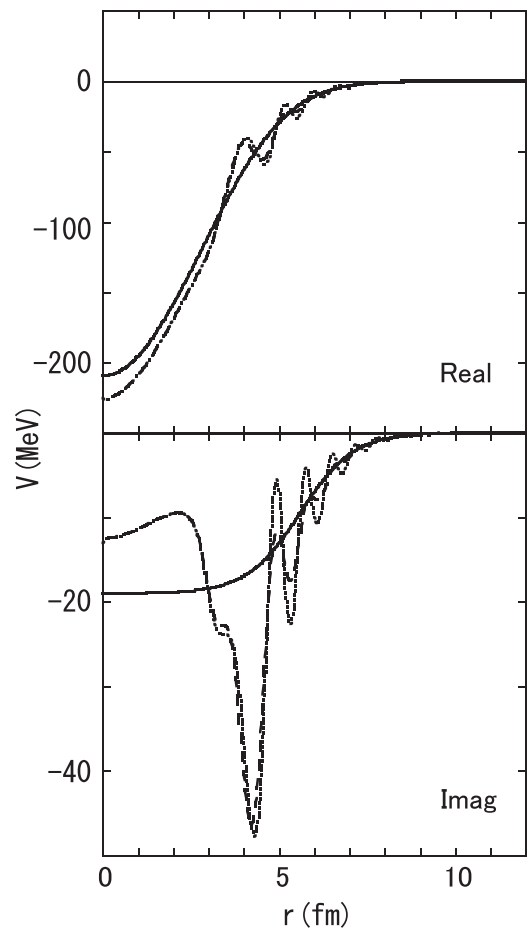

FIG. 1. For 330 MeV ^{16}O scattering from ^{12}C, the inverted potential fitting S_L in the presence of coupling to two states of ^{12}C. The solid line is for the bare potential (no coupling) and the more oscillatory dotted line is the inverted potential. The dashed line represents the potential at an earlier stage of the iterative inversion.
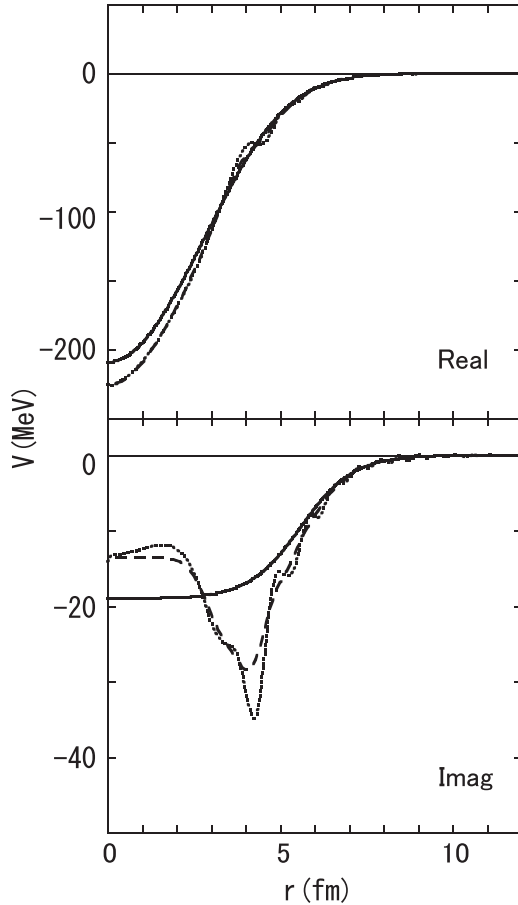
FIG. 2. The dotted line shows the inverted potential for coupling to 2^+ and 3^- states of ^{12}C with no direct coupling between these states. The dashed line is the inverted potential for coupling to just the 2^+ state of ^{12}C. The solid line is the bare potential (no coupling).

FIG. 3. For 330 MeV ^{16}O scattering from ^{12}C, the inverted potential fitting S_L for the full coupling to states of ^{12}C and ^{16}O. The solid line is for the bare potential (no coupling). The vertical scale for the imaginary part is different from the scale used in Figs. 1 and 2. The different imaginary bare potential for this case can be seen.

inversion process with fewer iterations, but the undulations are clearly lower in amplitude than those seen in Fig. 1. It is possible that direct coupling between the states generates some L dependence or generates interfering amplitudes of some kind. The undulations disappear when the 3^- state excitation is omitted, as seen in the dashed line in Fig. 2 which shows the DPP for the excitation of just the 2^+ state of ^{12}C. The undulations in the dotted line clearly arise from an interference between amplitudes, the amplitude corresponding to the 3^- state being very small. This can be seen from the small magnitude of the DPP for coupling to the 3^- state alone, which will be shown in Fig. 4 discussed below.

A comparison of the first three lines of Table I suggests that the 3^- state contributes much less to the DPP than the 2^+ state. Although the 3^- state does not contribute to the generation of the secondary rainbow, as seen in Fig. 2 of Ref. [1], it does make a small but non-negligible contribution to the angular distribution. This is consistent with its undularity effect on the radial shape of the DPP, as noted above. Although the coupling to the 3^- state generates clear interference effects, it is the coupling to the 2^+ state that is the key to generating the secondary rainbow.
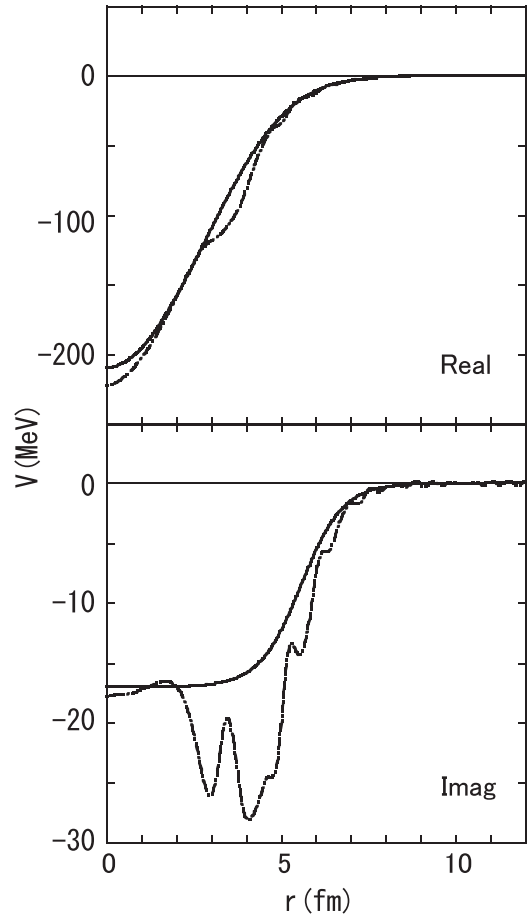
Some calculations were also carried out at 300 MeV incident energy. We noted above that, for 330 MeV incident energy, the DPP resulting from the simultaneous excitation of the 2^+ and 3^- states of ^{12}C was more undulatory when there was direct coupling between these two excitations than when there was no such direct coupling. This is not an artifact of the inversion process; the same increased undulatory character is also observed at an incident energy of 300 MeV when direct coupling is included between the excited state channels. The DPPs themselves at 300 MeV had the same general character as for 330 MeV and the direct coupling between excitations had almost no effect on the total reaction cross section, as was also the case at 330 MeV. Direct coupling between inelastic excitations may therefore be a source of undulations in nucleus-nucleus interactions in general, although the mechanism is obscure at present. This deserves both theoretical and phenomenological study.

IV. EXCITATION OF ^{16}O

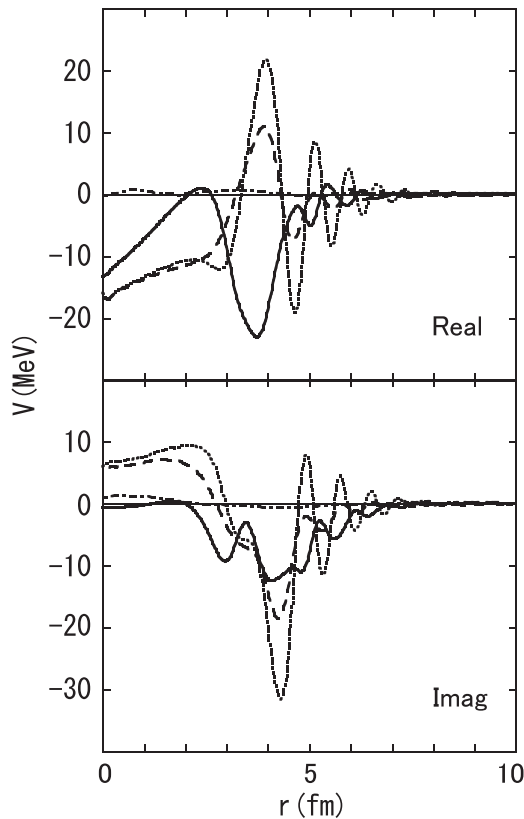Although instructive and crucial for the effects reported in Ref. [1], the DPPs due to the excitation of the two states of

FIG. 4. The DPPs implicit in Figs. 1, 2, and 3 are compared directly. The dotted line is the DPP for the excitation of both states of ^{12}C with direct coupling between them, the dashed line is the DPP when the direct coupling between the states of ^{12}C is omitted, and the solid line is the DPP for the "full" case, i.e., when the excitation of states of ^{16}O is added. The dash-dotted line is the small magnitude DPP due to the 3^- state of ^{12}C alone.

FIG. 5. Change in the elastic scattering S matrix S_L for coupling to the 2^+ and 3^- states of ^{12}C. The broken line is for the bare potential with no coupling and the solid line is with coupling. The upper panel shows $|S_L|$ and lower panel shows $\arg S_L$. The apparent discontinuity in $\arg S_L$ reflects the principal value of arctan, $-\pi \leqslant \arg S_L \leqslant \pi$

^{12}C are not the whole story. For the "full" case, the excitation of ^{16}O substantially modifies the DPPs; see Fig. 3: the real part now has substantial attraction around 4 fm, leading to the 10% increase in volume integral noted above, and the imaginary part loses almost all the emissivity within 3 fm, and is somewhat deeper towards the nuclear surface. The imaginary bare potential is shallower in the full case than in the other cases. This can easily be seen in Fig. 3. The imaginary bare potential also had smaller diffusivity, as can be seen with closer inspection of this figure.

In Fig. 4, which directly compares the DPPs implicit in the first three figures, the large attractive effect near 3.5 fm due to the excitation of ^{16}O is very apparent. From Fig. 2 of Ref. [1], the effect of the coupling to states of ^{16}O is mainly to fill in the deep minimum around $55°$. Figure 4 also presents the very small DPP due to coupling to just the 3^- state of ^{12}C. The DPP for the excitation of just the 2^+ state of ^{12}C (not shown) is slightly smoother than that when both states of ^{12}C are excited, with no direct coupling between them, as is clear from Fig. 2.

Insight into the contribution of the excitation of states of ^{16}O may be found by comparing the elastic channel S matrix for the cases with and without these excitations: S_L without

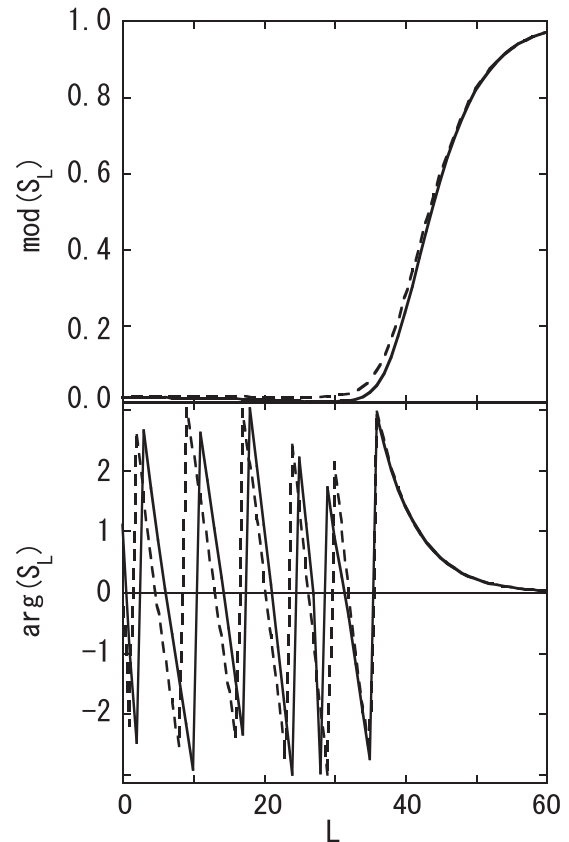the excitation of ^{16}O is shown in Fig. 5 and with that excitation in Fig. 6. The different behavior of $|S_L|$ for the bare potential (dashed lines) directly reflects the lesser depth and radial extent of the bare potential in the latter case. This corresponds to the difference in reaction cross sections when there is no coupling switched on: it is 1633.6 mb for the bare potential used when only the states of ^{12}C are excited and 1411.7 mb for the bare potential used in the calculations when the states of ^{16}O are also excited. Also, when comparing these figures, we see a much larger decrease in $|S_L|$ when ^{16}O coupling is included, and this is reflected in the increase in reaction cross section due to the coupling. This jumps from 15.6 mb when the states of ^{12}C are coupled to 70.4 mb when the states of ^{16}O are also included (see lines 3 and 6 of Table I). What is somewhat surprising is the relatively small increase in ΔJ_I. Since the bare imaginary potential is somewhat shallower and less diffuse in the full calculation, as is consistent with the behavior of $|S_L|$ as L approaches 60, it might be expected that the imaginary DPP would compensate for this. Indeed, the reduction in $|S_L|$ directly due to the coupling is greater for the full calculation, but the relatively small increase in ΔJ_I suggests that this is not entirely due to the imaginary DPP. The extra attraction around 3.5 fm may contribute to the absorption by attracting the nuclei into the absorptive potential. The reduction in $\arg S_L$ between
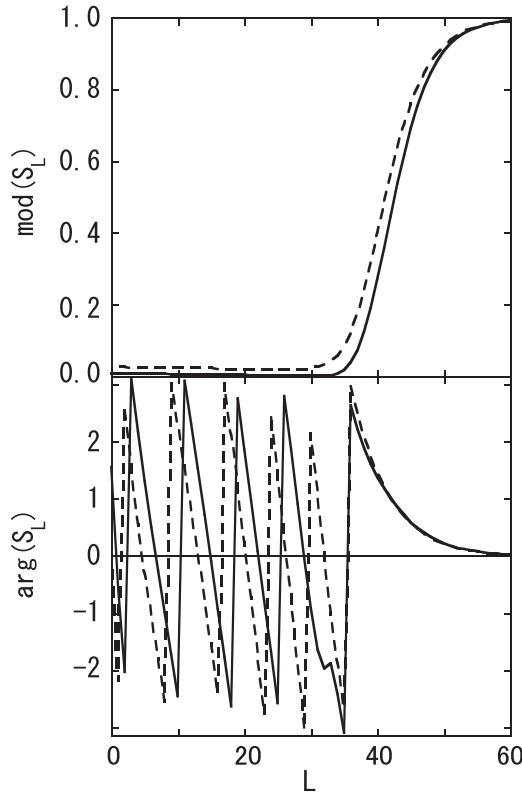
FIG. 6. Change in S_L for full calculations. The broken line is for the bare potential with no coupling and the solid line is for coupling to the states of ^{12}C and ^{16}O. $|S_L|$ is in the upper panel and arg S_L in the lower panel.

$L = 35$ and $L = 40$ that can be seen in Fig. 6 but is absent in Fig. 5 suggests a net repulsive effect in the surface which is not evident in Figs. 3 or 4.

In Fig. 7 we present the elastic scattering angular distributions for the full coupled channel calculation and for
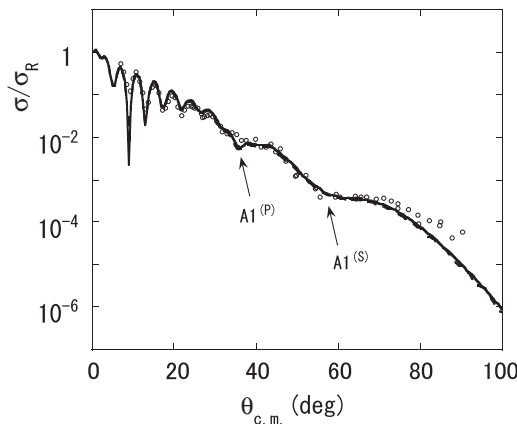

FIG. 7. Elastic scattering angular distribution for 330 MeV ^{16}O on ^{12}C. The circles represent the experimental measurements [15], the solid line is the coupled channel result, and the dotted line is for a single channel calculation with the sum of the bare potential and the full DPP. The primary and secondary Airy minima, A1^P and A1^S, are indicated by arrows.

single channel scattering due to the sum of the bare potential and the full DPP. They are evidently barely distinguishable. The experimental differential cross sections are included for comparison, indicating the primary and secondary Airy minima A1^P and A1^S [1].

V. DISCUSSION

It is often very instructive to examine the change in S_L, noting that $|S_L|$ is particularly related to the imaginary potential and arg S_L to the real part. Comparing Fig. 5, which shows the effect of the ^{12}C states alone, with Fig. 6, which shows the additional effect of the ^{16}O states, it appears somewhat surprising that it is the excitation of the ^{12}C states that has the major effect on correcting the elastic scattering angular distribution. It should be noted, comparing the dashed lines in these figures, that the significantly greater diffusivity (0.75 fm compared with 0.6 fm) and depth of the bare imaginary potential for the case without the ^{16}O excitation has greatly increased $1 - |S_L|$ for L between 40 and 60. The excitation of ^{16}O has a particularly large effect for this range of partial waves.

The DPP generated by the excitation of just the states of ^{12}C shows that strongly emissive regions can be generated in nuclear interactions by channel coupling. These do not, of course, lead to the breaking of the unitarity limit $|S_L| \leqslant 1$. Such regions sometimes appear in model independent fits in which the imaginary potential, over particular radial ranges, becomes small in magnitude or even positive; see for example Ref. [16]. It is likely that such emissivity indicates nonlocality and/or L dependence of the underlying DPP. It is interesting that the coupling to ^{16}O states almost removes the emissive region in this particular case, but nevertheless the potentiality for collective coupling to generate emissivity is clear.

An example that gives some insight into the very un-smooth shape of the resulting potential, and also shows what the inversion process must achieve for the full case, is shown in Fig. 8. This figure gives a close-up view of S_L for L from 20 to 36. The solid lines show the S_L to be fitted, and the dotted lines show S_L for an early stage of the iterative inversion process. The dashed lines correspond to a substantial change in the potential. For the final potential, the S_L would be indistinguishable from the solid line. The irregular form of S_L in this L region is presumably the result of interference between amplitudes the origin of which deserves further study.

There is one respect in which the present case conforms to expectations: the last two columns of Table I indicate that the increase in reaction cross section induced by the collective coupling exceeds the inelastic cross section. This behavior is not guaranteed and there are cases, e.g. [17], where inelastic processes increase the total cross section by much less than the magnitude of the inelastic cross section. That is even when the total cross section includes the additional inelastic cross sections. In the present case, when the coupling to the excited states of ^{16}O is included, the reaction cross section exceeds the cross section without coupling by substantially more than the total actual inelastic cross section to all the excited states; compare the difference between 15.6 and 14.8 mb on line 3
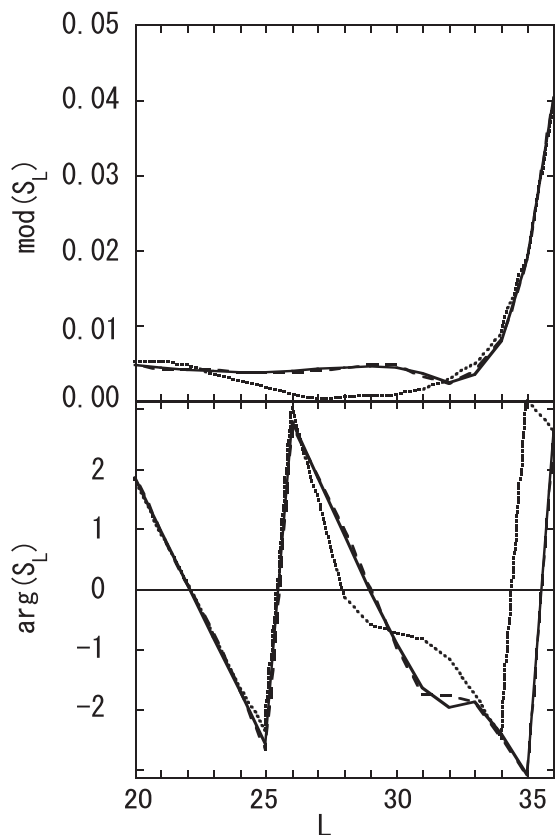
FIG. 8. For L between 20 and 35, S_L for the full calculation with $|S_L|$ in the upper panel and arg S_L in the lower panel. The dotted lines are for an earlier stage in the iterative inversion than the dashed lines. The solid lines give the CC S matrix to be inverted the "target" S matrix. The final converged potential gives S_L that is indistinguishable from the target S_L at this scale.

of Table I with that between 70.4 and 57.4 mb in line 6. The large value of Δ CS might be a result of the attractive effect around 3.5 fm drawing the projectile flux into the absorptive region. Recall that the bare potential for the full calculation has a significantly different imaginary term.

The excitation of just the collective 2^+ and 3^- states of ^{12}C, both with and without direct coupling between those states, generated rather small overall attraction or repulsion in the surface region, but did generate a deep absorptive feature in the imaginary potential together with a counterintuitive emissive region at a small separation distance. This, together with the inexact additivity of the local DPPs due to the 2^+ and 3^- states of ^{12}C without direct coupling between them, is strongly suggestive of dynamical nonlocality of the underlying DPP.

By contrast with the contribution of states of ^{12}C, for the case with full coupling the volume integral of the real potential was increased by about 10%, the largest increase being around the radius where the bare potential was about half the maximum depth. In the full case, the emissive region at a small separation distance almost completely disappeared.

It is probably true that, for many nucleus-nucleus combinations and energies, the radial range over which the potential can

be determined by elastic scattering data is much less than for the present case. For this reason, many discussions of the DPP due to projectile breakup, as calculated with the continuum discretized coupled-channel method [18–22], report the DPP mostly in the surface region. In fact, even ^{6}Li scattering is not that simple [17] and in that case, and quite generally for lighter "heavy ions," there is considerable nuclear overlap. As a result, the effect of coupling on the nuclear interaction extends over a radial range where the DPP may have a complicated form, with the effect on the real potential being very different from a uniform renormalization. We conclude from this, and also from the present calculations, that there are situations where the quality and angular range of the experimental data make the uniform renormalization of a folding model or global model potential an inappropriate phenomenological procedure. Correcting a folding model potential with a uniform normalizing factor can make sense in cases where only the surface region is relevant, but otherwise must be considered suspect. An appropriate phenomenology to exploit precise and wide angular range data would be to add a parameterized model independent correction to a global optical potential or a folding model potential. This has been done, for example by Khoa *et al.* [23].

The details of the interaction between arbitrary pairs of nuclei are beyond the reach of global models, since they will depend upon specific properties, such as the collectivities, of the particular interacting nuclei. The procedure employed in the present calculation provides a means of incorporating the particular characteristics of nuclei into a description of their elastic scattering, thus providing a means of going beyond the global models. We comment that Ref. [17] reveals the deficiency of the weighted trivially equivalent local potential, TELP, which has sometimes been employed as a means of calculating the DPP.

VI. SUMMARY

The discovery and explanation of a secondary rainbow in ^{16}O on ^{12}C elastic scattering around 300 MeV provides a conclusive example of the important contribution made by collective excitations to elastic scattering between nuclei. Specifically, Ref. [1] explained the occurrence of a secondary rainbow in the elastic scattering differential cross section. The scattering of ^{16}O on ^{12}C at 330 MeV is sensitive to the internuclear interaction well into the overlap region, affording an opportunity to study the DPP in a situation where little is known about it. Heretofore, DPPs have been evaluated in particular restricted cases: where one projectile is a light nucleus, where there is no coupling model that is justified by fitting data, or where the more limited TELP inversion procedure is applied. Here, we have applied IP $S_L \rightarrow V(r)$ inversion in a case where the excitation model is validated by its fit to scattering data. This reveals that the collective excitations generate a complicated DPP with both real and imaginary parts having radial forms that depart very far the bare potentials with uniform multiplicative factors. That is, for the real DPP in particular, the effects of the coupling could not be represented by a uniform renormalization of the folding model potential. It is reasonable to assume that this is a general property of collective contributions in strongly coupled

nucleus-nucleus collisions. By studying the DPPs for different combinations of coupled states we have found evidence for the dynamical nonlocality of the underlying DPP.

At present, a systematic understanding of the way in which collective excitations, and other channel coupling processes, modify the interaction between nuclei is still lacking. This is particularly true regarding the DPP where the interacting nuclei substantially overlap; here, little is known apart from some cases involving light projectiles, $A \leqslant 6$. Such dynamically generated interactions, and the manner in which they depend upon the particular properties of the interacting nuclei, are accessible by combining coupled channels calculations

with S-matrix inversion, as we have demonstrated here for strongly overlapping composite nuclei.

[1] S. Ohkubo and Y. Hirabayashi, Phys. Rev. C **89**, 051601 (2014).

[2] S. Ohkubo and Y. Hirabayashi, Phys. Rev. C **89**, 061601 (2014).

[3] H. Feshbach, Ann. Phys. (NY) **5**, 357 (1958); **19**, 287 (1962).

[4] G. R. Satchler, *Direct Nuclear Reactions* (Clarendon Press, Oxford, 1983).

[5] G. H. Rawitscher, Nucl. Phys. A **475**, 519 (1987).

[6] R. S. Mackintosh and N. Keeley, Phys. Rev. C **90**, 044601 (2014).

[7] N. Keeley and R. S. Mackintosh, Phys. Rev. C **90**, 044602 (2014).

[8] R. S. Mackintosh and S. G. Cooper, Nucl. Phys. A **494**, 123 (1989).

[9] R. S. Mackintosh and S. G. Cooper, Phys. Rev. C **47**, 1716 (1993).

[10] R. S. Mackintosh and A. M. Kobos, Phys. Lett. B **116**, 95 (1982).

[11] S. G. Cooper and R. S. Mackintosh, Inverse Problems **5**, 707 (1989).

[12] V. I. Kukulin and R. S. Mackintosh, J. Phys. G: Nucl. Part. Phys. **30**, R1 (2004).

[13] R. S. Mackintosh, arXiv:1205.0468.

[14] R. S. Mackintosh, Scholarpedia **7**, 12032 (2012).

[15] A. S. Dem'yanova *et al.*, IAEA Database Exfor, http://www-nds.iaea.org/exfor/

[16] M. Ermer, H. Clement, P. Grabmayr, G. J. Wagner, L. Friedrich, and E. Huttel, Phys. Lett. B **188**, 17 (1987).

[17] D. Y. Pang and R. S. Mackintosh, Phys. Rev. C **84**, 064611 (2011).

[18] G. H. Rawitscher, Phys. Rev. C **9**, 2210 (1974).

[19] J. P. Farrell, Jr., C. M. Vincent, and N. Austern, Ann. Phys. (NY) **96**, 333 (1976).

[20] M. Yahiro, N. Nakano, Y. Iseri, and M. Kamimura, Prog. Theor. Phys. **67**, 1467 (1982).

[21] N. Austern, Y. Iseri, M. Kamimura, M. Kawai, G. Rawitscher, and Y. Yahiro, Phys. Rep. **154**, 125 (1987).

[22] Y. Sakuragi, M. Yahiro, and M. Kamimura, Prog. Theor. Phys. Suppl. **89**, 136 (1986).

[23] D. T. Khoa, G. R. Satchler, and W. von Oertzen, Phys. Rev. C **51**, 2069 (1995).